# Supporting information

## Investigating the Mechanism of Propylene Epoxidation over Halogen (X=F, Cl, Br, I) Modified $Cu_2O(110)$ Surfaces: A Theoretical Study

Lingyun Zhou,*[a] Zhu Wen,[a] Leyuan Cui,[b] Guangxu Yang,[a] Yingchun Luo,[a] Yadian Xie,[a] Can Cui,[a] Chunyan Li,[a] Gang Fu,*[b]

[a]School of Chemical Engineering, Key Laboratory of Low-Dimensional Materials and Big Data, Guizhou Minzu University, Guizhou Provincial Key Laboratory of Low Dimensional Materials and Environmental and Ecological Restorations, Guizhou, Guiyang 550025, China;

[b]State Key Laboratory of Physical Chemistry of Solid Surfaces, Department of Chemistry, College of Chemistry and Chemical Engineering, Xiamen University, Xiamen 361005, China.

*Corresponding authors. E−mail: lyzhou@gzmu.edu.cn; gfu@xmu.edu.cn (G. Fu)

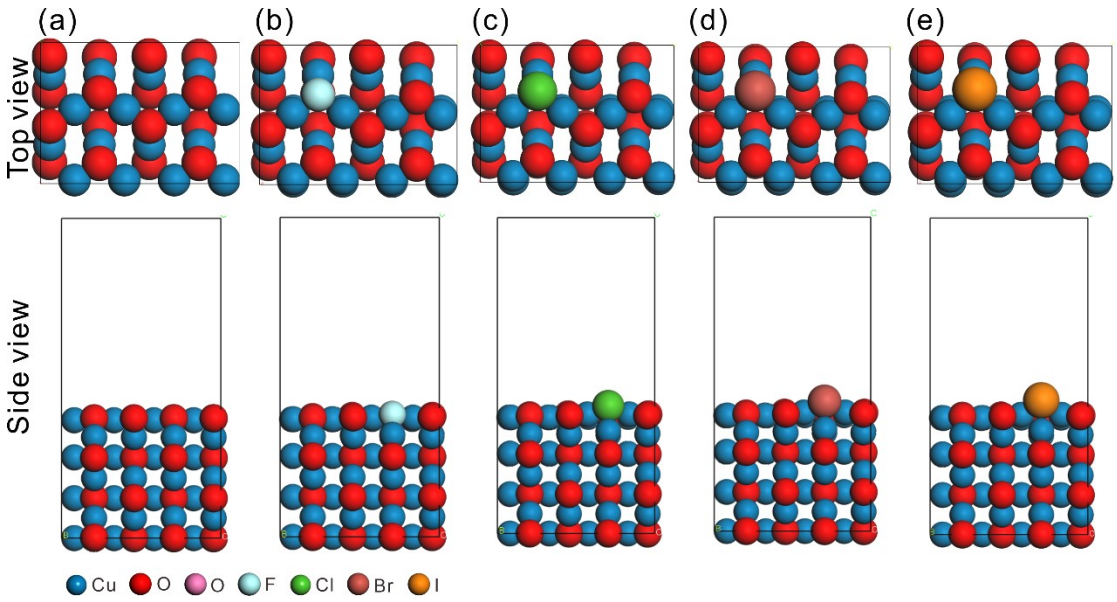


**Fig. S1.** The top view and side view of the computational models. (a) $Cu_2O(110)$, (b) F-$Cu_2O(110)$, (c) Cl-$Cu_2O(110)$, (d) Br-$Cu_2O(110)$, (e) I-$Cu_2O(110)$.

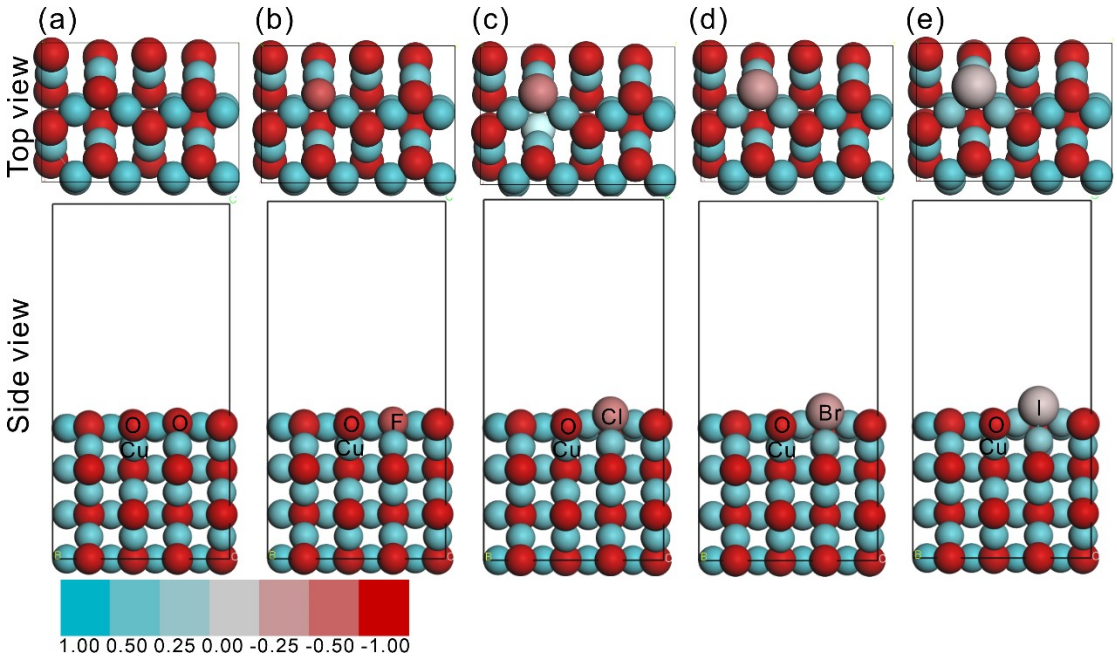


**Fig. S2.** Bader charge analysis of pristine $Cu_2O(110)$, F-$Cu_2O(110)$, Cl-$Cu_2O(110)$, Br-$Cu_2O(110)$ and I-$Cu_2O(110)$ surfaces. The color gradient indicated the magnitude of Bader charge.

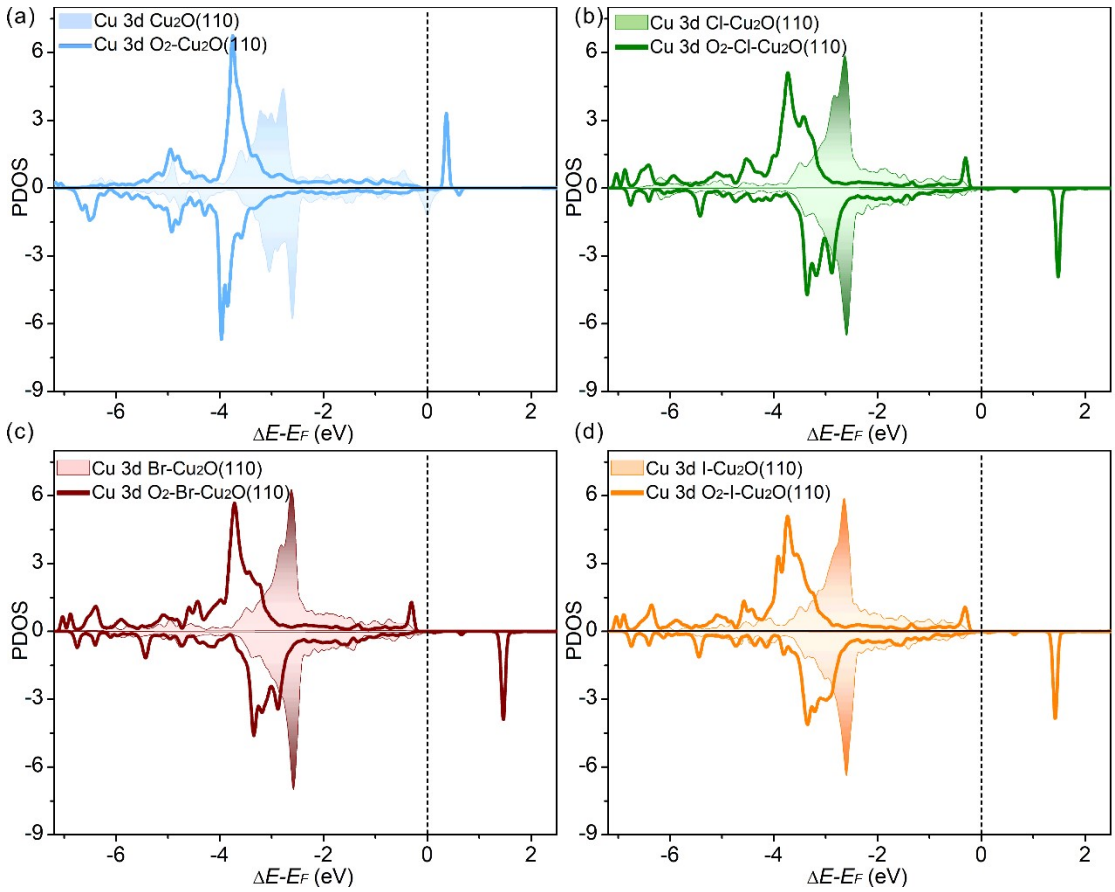


**Fig. S3.** The projected density of states (PDOS) of the 3d orbitals of surface Cu atoms directly coordinated with X before and after $O_2$ adsorption (a) $Cu_2O(110)$, (b) Cl-$Cu_2O(110)$, (c) Br-$Cu_2O(110)$ and (d) I-$Cu_2O(110)$

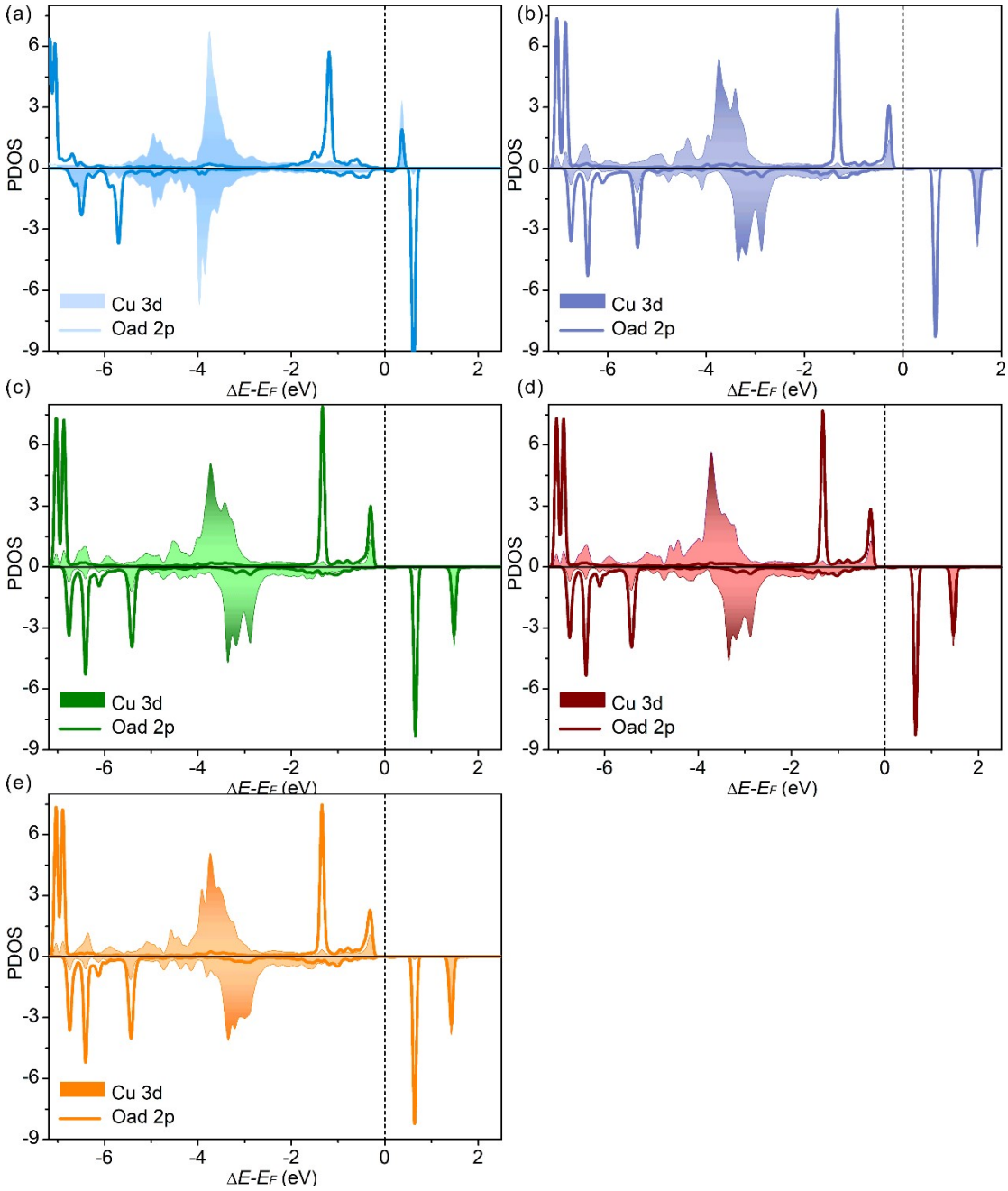


**Fig. S4.** The PDOS of the 3d orbitals of surface Cu atoms directly coordinated with X after $O_2$ adsorption and the 2p orbitals of the adsorbed $O_2$, (a) $Cu_2O(110)$, (b) F-$Cu_2O(110)$, (c) Cl-$Cu_2O(110)$, (d) Br-$Cu_2O(110)$ and (e) I-$Cu_2O(110)$.

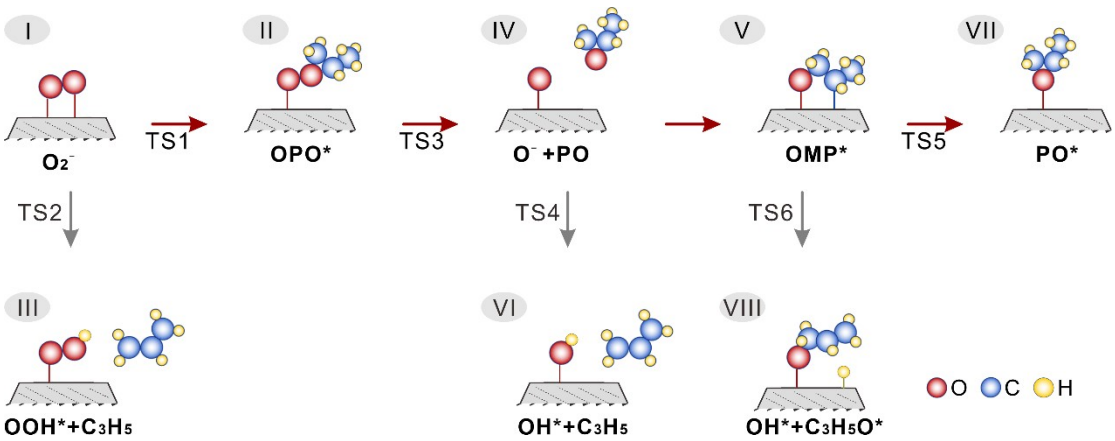


**Fig. S5.** Proposed reaction network of propylene oxidation by adsorbed $O_2$. (I) adsorbed $O_2$; (II) peroxirane intermediate; (III) allyl intermediate; (IV) adsorbed O atom; (V) OMP* intermediate; (VI) allyl intermediate; (VII) adsorbed PO*; (VIII) allylic oxygen intermediate; (TS1) oxygen insertion; (TS2) α-H abstraction; (TS3) O-O bond cleavage; (TS4) α-H abstraction; (TS5) ring closing; (TS6) α-H abstraction.

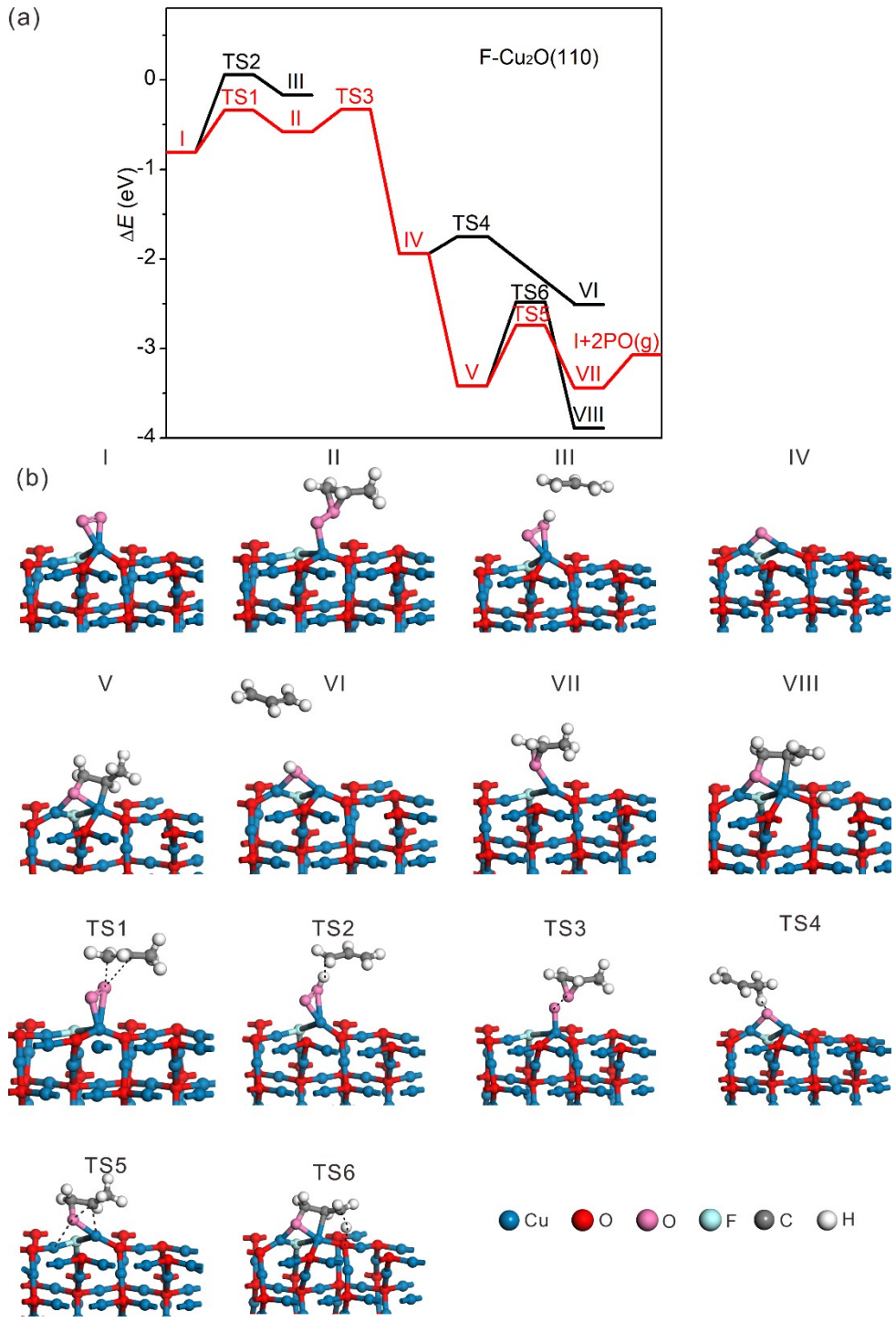


**Fig. S6.** The reaction of two propylene molecules with adsorbed $O_2$ on F-$Cu_2O$ (110) surface: (a) potential energy profiles of propylene epoxidation from DFT; (b) optimized structures of intermediates and transition states involved in propylene epoxidation.

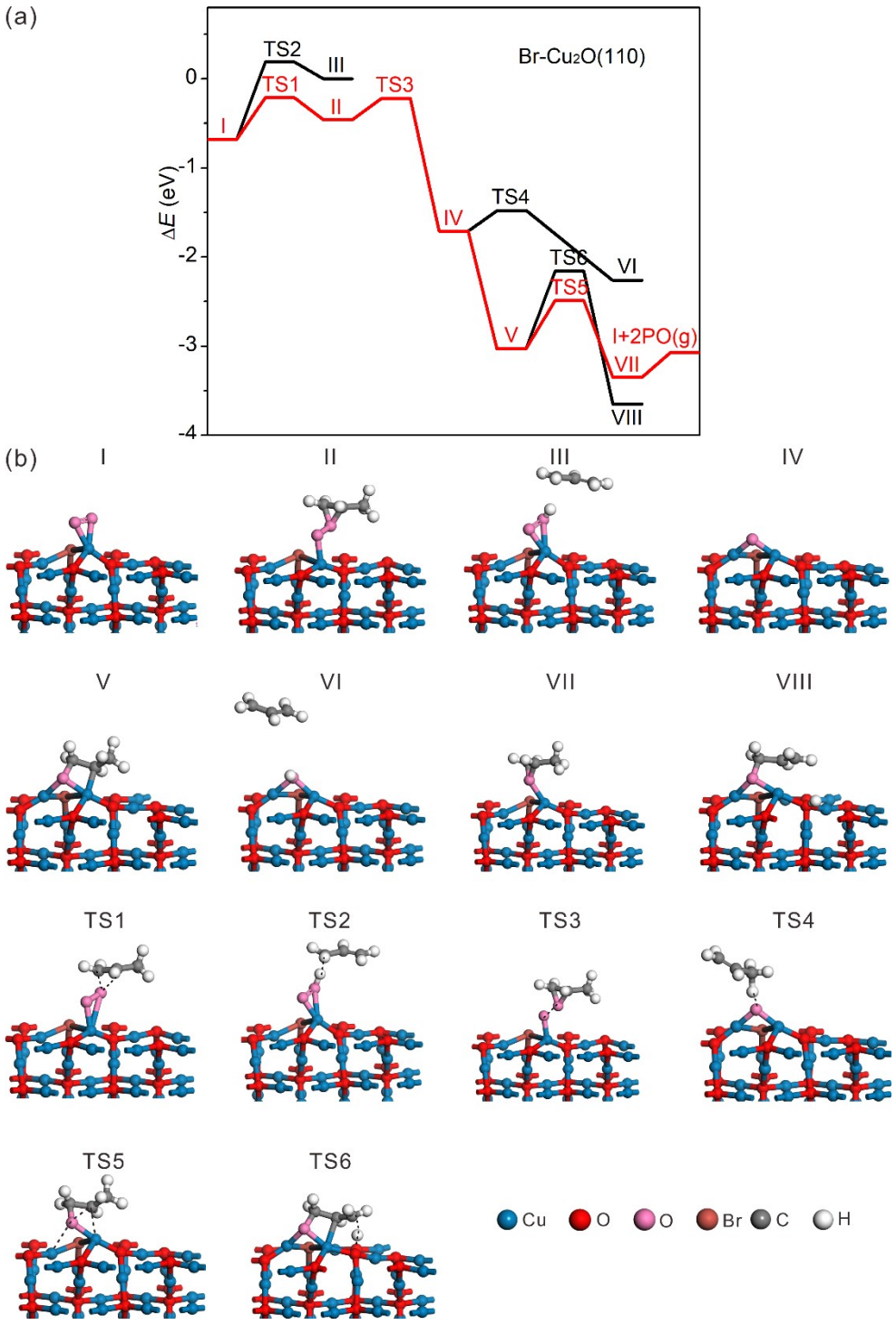


**Fig. S7.** The reaction of two propylene molecules with adsorbed $O_2$ on Br-$Cu_2O$ (110) surface: (a) potential energy profiles of propylene epoxidation from DFT; (b) optimized structures of intermediates and transition states involved in propylene epoxidation.

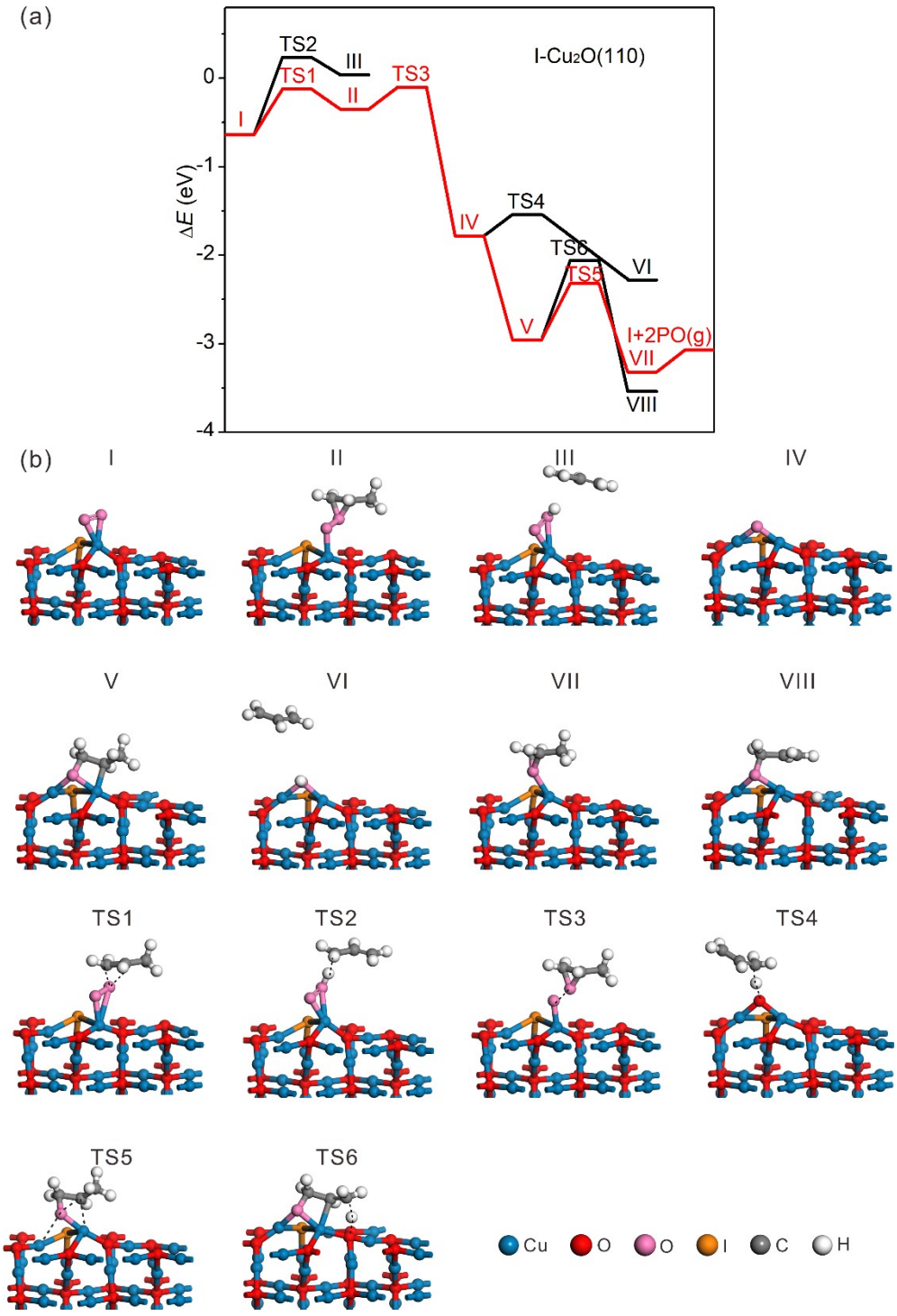


**Fig. S8.** The reaction of two propylene molecules with adsorbed $O_2$ on I-$Cu_2O$ (110) surface: (a) potential energy profiles of propylene epoxidation from DFT; (b) optimized structures of intermediates and transition states involved in propylene epoxidation.

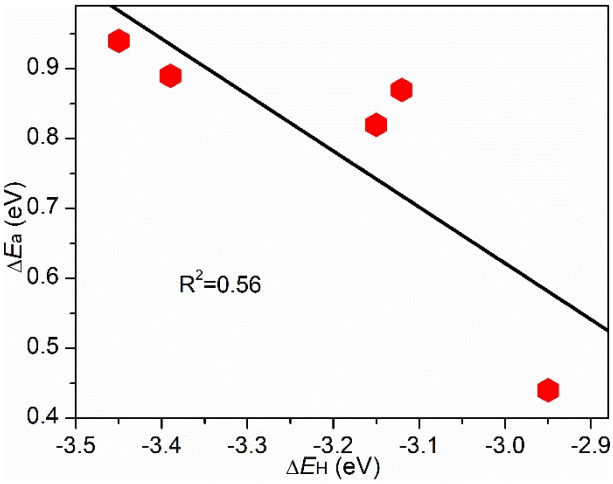


**Fig. S9.** The linear relationship between the hydrogen affinity ($\Delta E_H$) of lattice oxygen species ($O^{2-}$) and the energy barriers ($\Delta E_a$) for the α-H abstraction.

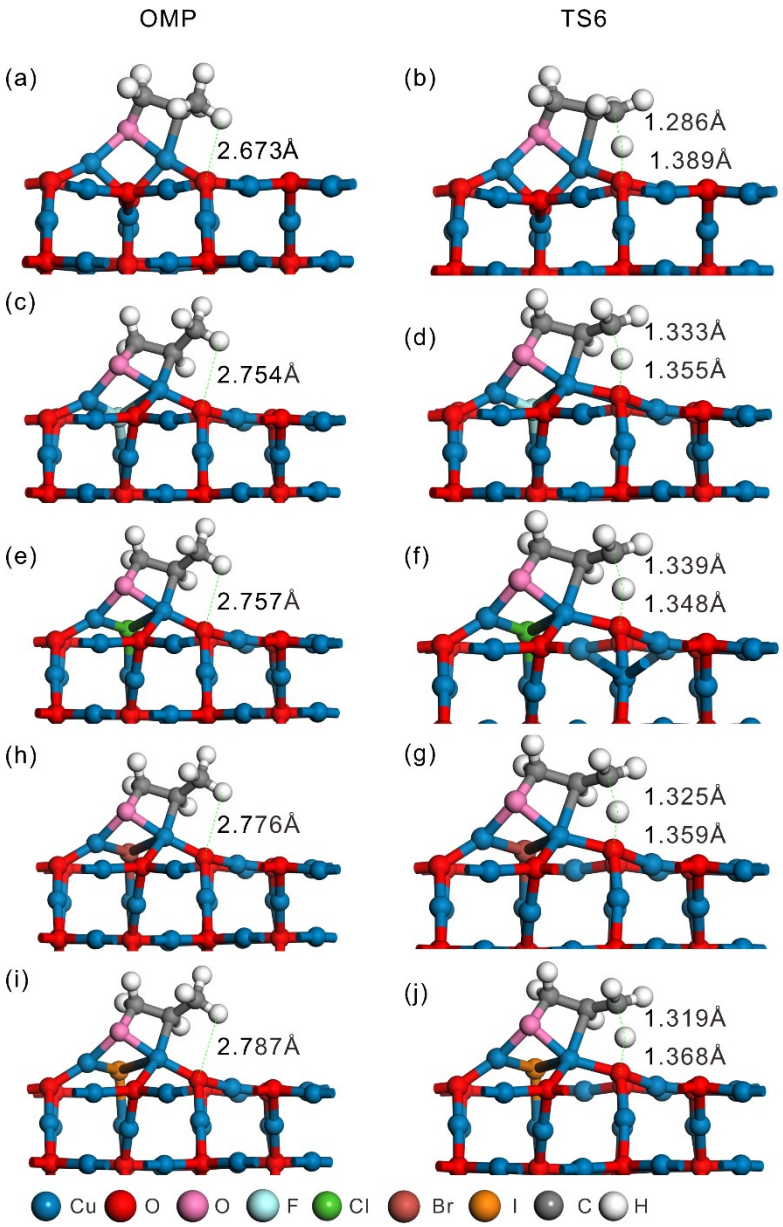


**Fig. S10.** The bond lengths involved in α-H abstraction reaction: (a)-(b) $Cu_2O(110)$, (c)-(d) F-$Cu_2O(110)$, (e)-(f) Cl-$Cu_2O(110)$, (h)-(g) Br-$Cu_2O(110)$ and (i)-(j) I-$Cu_2O(110)$ surfaces.

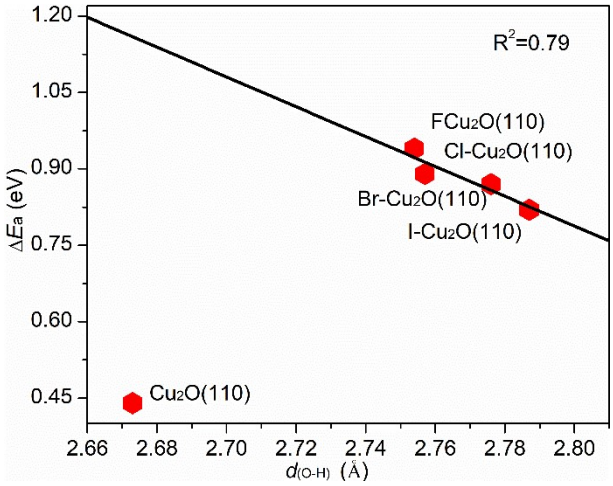


**Fig. S11.** The plot of $d_{(OH)}$ versus $\Delta E_a$ for α-H abstraction.

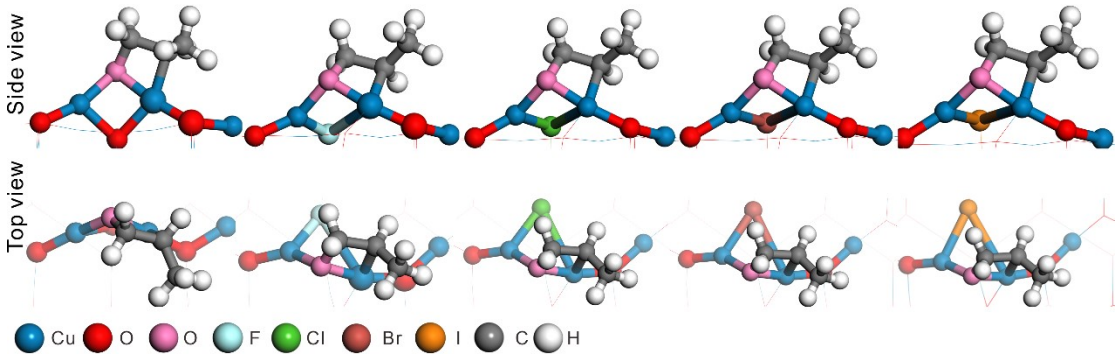


**Fig. S12.** The side view and top view of the OMP* on $Cu_2O(110)$, F-$Cu_2O(110)$, Cl-$Cu_2O(110)$, Br-$Cu_2O(110)$ and I-$Cu_2O(110)$ surfaces.

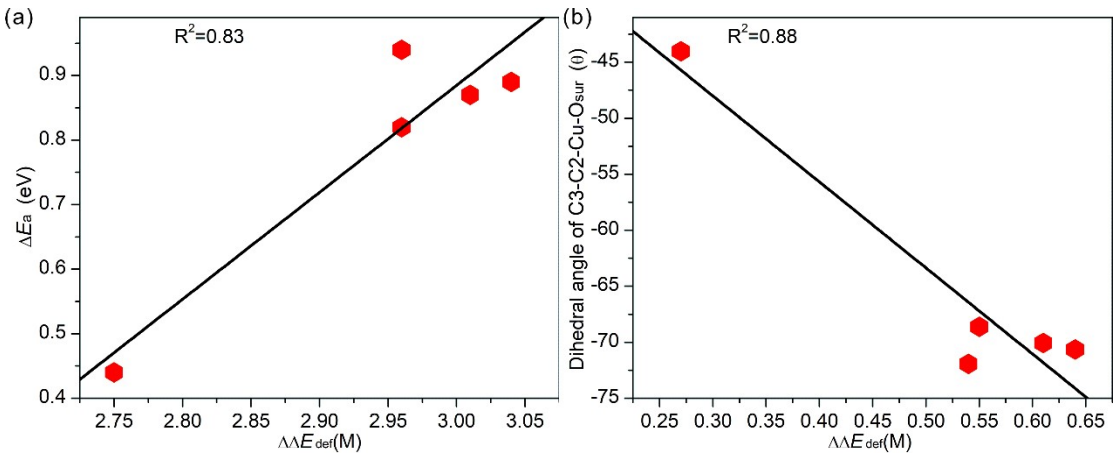


**Fig. S13.** (a) The linear relationship between $\Delta\Delta E_{def}$(M) and $\Delta E_a$ for α-H abstraction. (b) The plot of $\Delta\Delta E_{def}$(M) versus the dihedral angles D(C3-C2-Cu-$O_{sur}$) of OMP*.

**Table S1**

Summary of the adsorption energies ($\Delta E_{ad}$), O-O bond lengths and Bader charges of $O_2$ adsorption on $Cu_2O$(110) and halogen modified $Cu_2O$(110) surfaces.

| Surface | $\Delta E_{ad}$ (eV) | $d_{(O=O)}$ (Å) | $d_{(Cu-O)}$ (Å) | Bader Charge (\|e\|) |
|---|---|---|---|---|
| $Cu_2O$(110) | -0.57 | 1.274 | 2.123 | -0.15 |
| | | | 2.105 | -0.10 |
| F-$Cu_2O$(110) | -0.81 | 1.319 | 1.945 | -0.20 |
| | | | 1.989 | -0.18 |
| Cl-$Cu_2O$(110) | -0.68 | 1.318 | 1.944 | -0.20 |
| | | | 2.003 | -0.18 |
| Br-$Cu_2O$(110) | -0.68 | 1.316 | 1.946 | -0.20 |
| | | | 2.014 | -0.18 |
| I-$Cu_2O$(110) | -0.64 | 1.316 | 1.945 | -0.21 |
| | | | 2.030 | -0.18 |

**Table S2**

Summary of the bond length $d_{(Cu\text{-}X)}$, Bader Charge of Cu atoms directly coordinated with X in the top and sub layers of halogen modified $Cu_2O(110)$ surface and the adsorption energy ($\Delta E_{ad}$) of X on the vacancy site of the $Cu_2O(110)$ surface.

| Surface | [a]$d_{(Cu\text{-}X)}$ (Å) | [b]$d_{(Cu\text{-}X)}$ (Å) | [a]Bader Charge (\|e\|) | [b]Bader Charge (\|e\|) | $\Delta E_{ad}$ (eV) |
|---|---|---|---|---|---|
| $Cu_2O(110)$ | 1.805<br>1.805 | 1.807 | +0.64<br>+0.64 | +0.53 | -5.96 |
| F-$Cu_2O(110)$ | 1.928<br>1.928 | 1.958 | +0.57<br>+0.57 | +0.51 | -5.54 |
| Cl-$Cu_2O(110)$ | 2.158<br>2.158 | 2.193 | +0.51<br>+0.51 | +0.46 | -4.28 |
| Br-$Cu_2O(110)$ | 2.290<br>2.290 | 2.331 | +0.47<br>+0.47 | +0.42 | -3.91 |
| I-$Cu_2O(110)$ | 2.446<br>2.446 | 2.493 | +0.41<br>+0.41 | +0.37 | -3.29 |

[a]Cu atoms directly coordinate with X in the top layer, [b]Cu atoms directly coordinate with X in the sub layer.

**Table S3**

Summary of the reaction energies of each elementary step in DEP on pristine $Cu_2O(110)$ and halogen modified $Cu_2O(110)$ surfaces.

| | $Cu_2O(110)$ | F-$Cu_2O(110)$ | Cl-$Cu_2O(110)$ | Br-$Cu_2O(110)$ | I-$Cu_2O(110)$ |
|---|---|---|---|---|---|
| I | -0.57 | -0.81 | -0.68 | -0.68 | -0.64 |
| TS1 | 0.12(0.69) | -0.34(0.47) | -0.23(0.45) | -0.21(0.47) | -0.12(0.52) |
| II | -0.55 | -0.58 | -0.46 | -0.46 | -0.35 |
| TS2 | 0.44(1.01) | 0.06(0.87) | 0.18(0.86) | 0.19(0.87) | 0.24(0.88) |
| III | 0.16 | -0.17 | 0.00 | 0.00 | 0.04 |
| TS3 | -0.15(0.40) | -0.33(0.25) | -0.23(0.23) | -0.22(0.24) | -0.10(0.25) |
| IV | -1.92 | -1.94 | -1.64 | -1.71 | -1.78 |
| V | -2.68 | -3.42 | -3.02 | -3.03 | -2.96 |
| TS4 | -1.53(0.39) | -1.75(0.19) | -1.40(0.24) | -1.48(0.23) | -1.54(0.24) |
| VI | -2.14 | -2.51 | -2.18 | -2.26 | -2.28 |
| TS5 | -2.19(0.49) | -2.74(0.68) | -2.51(0.51) | -2.49(0.54) | -2.32(0.64) |
| VII | -3.55 | -3.44 | -3.33 | -3.35 | -3.32 |
| TS6 | -2.24(0.44) | -2.48(0.94) | -2.13(0.89) | -2.16(0.87) | -2.14(0.82) |
| VIII | -3.54 | -3.89 | -3.81 | -3.65 | -3.54 |

**Table S4**

Decomposition of the energies of OMP* on pristine $Cu_2O(110)$ and halogen modified $Cu_2O(110)$ surfaces.

| | $Cu_2O(110)$ | F-$Cu_2O(110)$ | Cl-$Cu_2O(110)$ | Br-$Cu_2O(110)$ | I-$Cu_2O(110)$ |
|---|---|---|---|---|---|
| $\Delta E_{def}$(M) | 2.48 | 2.41 | 2.40 | 2.40 | 2.42 |
| $\Delta E_{def}$(S) | 1.95 | 1.41 | 1.54 | 1.54 | 1.59 |
| $\Delta E_{int}$ | -7.11 | -7.25 | -6.96 | -6.96 | -6.97 |
| $\Delta E$ | -2.68 | -3.42 | -3.02 | -3.03 | -2.96 |

**Table S5**

Decomposition of the energies of TS6 on pristine $Cu_2O(110)$ and halogen modified $Cu_2O(110)$ surfaces.

| | $Cu_2O(110)$ | F-$Cu_2O(110)$ | Cl-$Cu_2O(110)$ | Br-$Cu_2O(110)$ | I-$Cu_2O(110)$ |
|---|---|---|---|---|---|
| $\Delta E_{def}$(M) | 2.75 | 2.96 | 3.04 | 3.01 | 2.96 |
| $\Delta E_{def}$(S) | 1.89 | 1.42 | 1.57 | 1.54 | 1.5 |
| $\Delta E_{int}$ | -6.88 | -6.87 | -6.78 | -6.71 | -6.6 |
| $\Delta E$ | -2.24 | -2.48 | -2.17 | -2.16 | -2.14 |

**Table S6**

The energy difference between TS6 and OMP* on pristine $Cu_2O(110)$ and halogen modified $Cu_2O(110)$ surfaces.

| | $Cu_2O(110)$ | F-$Cu_2O(110)$ | Cl-$Cu_2O(110)$ | Br-$Cu_2O(110)$ | I-$Cu_2O(110)$ |
|---|---|---|---|---|---|
| $\Delta\Delta E_{def}$(M) | 0.27 | 0.54 | 0.64 | 0.61 | 0.55 |
| $\Delta\Delta E_{def}$(S) | -0.06 | 0.01 | 0.06 | 0.00 | -0.09 |
| $\Delta\Delta E_{int}$ | 0.23 | 0.39 | 0.18 | 0.26 | 0.37 |
| $\Delta E_a$ | 0.44 | 0.94 | 0.89 | 0.87 | 0.82 |